2019 IEEE 58th Conference on Decision and Control (CDC)
Palais des Congrès et des Expositions Nice Acropolis
Nice, France, December 11-13, 2019

Distributed Model Predictive Control for Autonomous Droop-Controlled Inverter-Based Microgrids

Sean Anderson, Patricia Hidalgo-Gonzalez, Roel Dobbe, and Claire J. Tomlin

Abstract— **Microgrids must be able to restore voltage and frequency to their reference values during transient events; inverters are used as part of a microgrid's hierarchical control for maintaining power quality. Reviewed methods either do not allow for intuitive trade-off tuning between the objectives of synchronous state restoration, local reference tracking, and disturbance rejection, or do not consider all of these objectives. In this paper, we address all of these objectives for voltage restoration in droop-controlled inverter-based islanded microgrids. By using distributed model predictive control (DMPC) in series with an unscented Kalman Filter (UKF), we design a secondary voltage controller to restore the voltage to the reference in finite time. The DMPC solves a reference tracking problem while rejecting reactive power disturbances in a noisy system. The method we present accounts for non-zero mean disturbances by design of a random-walk estimator. We validate the method's ability to restore the voltage in finite time via modeling a multi-node microgrid in Simulink.**

I. Introduction

A microgrid (MG) operating in islanded mode must be able to maintain the power quality of the system, including restoring voltage and frequency to the nominal values [1], [2]. The restoration is necessary as changes in load cause steady-state offsets. In the case of inverter-based microgrids, the inverters provide the control action for maintaining power quality [3]. Inverter-based microgrids have at least one inverter in grid-forming mode. Inverters are grid-forming when they supply the signal for the frequency and voltage. A grid-forming inverter is known as a voltage source inverter (VSI). Multiple VSIs can be paralleled in one MG and any remaining inverters will be in a mode such that they follow the grid signal [4]. Under transient conditions, voltage and frequency must be restored to the nominal value and kept within specific operating bounds. As a nodal network – where an inverter represents a node – the problem becomes how to restore the states, namely the voltage and frequency at each node, to the references. Stability is defined here as the ability of the (controlled) system to remain within operating bounds after being subjected to disturbances [5]. For instance, voltage must be maintained within specified limits despite reactive power disturbances. The networked system presents a challenge to control because the dynamical coupling between the states dictates that not just the local state must be considered, but neighboring states as well.

In microgrids, the control hierarchy consists of three layers [6]–[8]. Primary control is the fastest control and is traditionally a proportional control. Secondary control encompasses restoring states to their nominal values and can include finding setpoints for primary control. Last, tertiary control generally solves economic dispatch problems and chooses control setpoints for the lower layers.

Secondary and tertiary control use a spectrum of centralized, decentralized, and distributed methods. Centralized methods use a central controller that has knowledge of every node [9]. Due to the full knowledge of the system, centralized methods are able to achieve the global optimum in optimal control formulations. Drawbacks include a single point of failure, large communication requirements, and lack of modularity [10].

In fully decentralized approaches, the control is localized and the individual systems are taken to be decoupled dynamically [11]–[13]. The interaction between nodes is characterized as disturbances to the individual systems. In [11], an effective decentralized control method is proposed for distribution grids. While effective in some power systems, local controllers are not always robust, leading to cascading divergence of the local states across a network [1].

Distributed methods only have computation at each node and communicate with the respective neighbors [14]. Unlike centralized approaches, these do not necessarily lead to a globally optimal solution with respect to a defined cost function (i.e. transient response time, power sharing, synchronicity). While distributed approaches are more robust to failures due to the distributed computation and control as well as more adaptability to network changes, issues of convergence, stability, and communication requirements are prevalent [15], [16]. A method known as distributed model predictive control (DMPC) solves an optimal control problem at each node [17]. The problem at each node is solved as a finite horizon control problem in a receding horizon while communicating with neighboring nodes in the network at a specified sampling rate [18]. DMPC is shown to reduce computational complexity relative to centralized control while generally ensuring better robustness to neighbors' deviations from nominal in comparison with decentralized control [14], [19].

A number of distributed methods for secondary voltage and frequency control of islanded, inverter-based microgrids

Sean Anderson is with Engineering Science, University of California, Berkeley, CA 94720, USA, and New Sun Road P.B.C, Richmond, CA 94804, USA. sean.anderson@berkeley.edu

Patricia Hidalgo-Gonzalez is with the Department of Electrical Engineering and Computer Sciences and the Energy and Resources Group, University of California, Berkeley, CA 94720, USA. patricia.hidalgo.g@berkeley.edu

Roel Dobbe is with AI Now Institute, New York University, New York, NY 10003, USA. roel@ainowinstitute.org

Claire J. Tomlin is with the Department of Electrical Engineering and Computer Sciences, University of California, Berkeley, CA 94720, USA. tomlin@berkeley.edu

978-1-7281-1398-2/19/$31.00 ©2019 IEEE

has been proposed [10], [20]–[22]. As this work focuses on secondary voltage control, we omit review of secondary frequency control. While each work takes a unique approach, they are all working with the same underlying physical dynamics. A key differentiating feature between these works is whether the dynamics model used directly considers the dynamical coupling with neighboring nodes. In [20], a continuous-time secondary voltage controller is designed such that the input does not depend on the neighbors' voltages. While the analysis indicates that this is stable in the sense of Lyapunov, the neighbors' states are not explicitly included and thus the restoration of the voltages is not necessarily synchronized nor optimal. The work presented in [21] uses a nonlinear controller that minimizes the local voltage neighborhood tracking error; the premise is that only one node of the network has knowledge of the voltage reference. A model with explicit dynamical coupling is used in the controller to restore the voltage at each node in finite time. While effective, tuning the gains in this nonlinear controller for transient response performance is non-intuitive. A DMPC approach is presented in [22]. As in [21], the voltage reference is only known at one node in the network. The method synchronously restores the voltage in finite time. However, the model does not explicitly account for the dynamical coupling. This type of model-mismatch often results in steady-state error in MPC formulations without integral action. The relevance of dynamic coupling of subsystems when used in DMPC is shown in [23]. Lastly, in [10], a sliding mode cooperative controller is proposed. This addresses voltage restoration synchronization but mainly focuses on robust control; this is included as a relevant distributed method although the dynamical modeling of the system is quite different.

In this paper, we develop a DMPC that simultaneously takes into account dynamical coupling (enabling synchronized restoration), finite time voltage restoration, and the presence of noisy disturbances. We start by modeling the voltage dynamics as a first order system with dynamical coupling between nodes. The continuous dynamics are discretized for the purposes of the DMPC. The DMPC cost function allows for intuitive transient response tuning and trade-off between local voltage restoration, synchronous restoration, and input control action. In order to address model-mismatch, we design a distributed state estimator so that noisy, non-zero mean disturbances can be rejected. The integral action is not inherent to the DMPC and must be introduced by solving for the reference input control. This can be solved analytically for the given dynamics instead of having to solve a least squares problem.

The contributions of this work are two-fold:

1) We present an MPC scheme for secondary control that uses the nonlinear voltage dynamics not previously used in DMPC; only secondary voltage control is addressed. The chosen dynamics model allows for the network's states to converge synchronously. By introducing a novel method to compute the state and input reference, offset-free tracking is provided; this functions in conjunction with a distributed estimator.

2) We design a distributed state estimator that estimates the local voltage and an unknown noisy reactive power disturbance. The disturbance estimate evolves as a random walk to provide a non-zero mean estimate of the true disturbance. The disturbance could be a biased measurement of the reactive load or an unaccounted-for device with reactive power injection/consumption.

II. Microgrid Modeling

A. Network Model

1) Graph Theory and Power System Network: The network of a multi-agent system can be described as an undirected graph $\mathcal{G} = (\mathcal{V}, \mathcal{E}, A)$ where $\mathcal{V} = \{1, .., N\}$ is a non-empty set of N nodes that generally may have distributed generation (DG), $\mathcal{E}$ is the set of edges representing the line impedances, and A is the adjacency matrix where $a^{m,m} = 0$ and $a^{m,n} = 1$ for all connected nodes $m \neq n$. In alignment with convention, we represent the line impedances, Z, as the admittance matrix Y ($Z = Y^{-1}$) where $Y^{m,n} = G^{m,n} + jB^{m,n}$ $\forall(m, n)$ where $j = \sqrt{-1}$ [24]. The diagonal degree matrix, D, can then be defined as $d^{m,m} = \sum_{n\in\mathcal{N}_m} a^{m,n}$ where $\mathcal{N}_m := \{n|(m, n) \in \mathcal{E}\}$. Here $\mathcal{N}_m$ denotes the electrically connected neighborhood of the node m. In general, there exists a communication neighborhood, $\mathcal{N}_{\mathcal{C}_m}$, which indicates node-to-node communication ability. For this work, we take the communication and electrically connected neighborhoods to be the same. The self-susceptances are defined to be $B^{m,m} = \sum_{n\in\mathcal{N}_m} B^{m,n}$ [21]. Finally, the Laplacian matrix is defined to be $L = D - A$. The adjacency and Laplacian matrices can be used for representing the general connectivity of the subsystems. In the distributed context, the adjacency matrix is useful for encoding information matrix-wise; however, the entire matrix will not be used at one node if the communication neighborhood does not equal the full set of the nodes.

The canonical equations describing power injection at a node m, [24] are:

$$\hat{P}^m = \sum_{n\in\mathcal{N}_m} V^m V^n |Y^{m,n}| cos(\theta^{m,n} + \delta^n - \delta^m), \quad (1)$$

$$\hat{Q}_m = -\sum_{n\in\mathcal{N}^m} V^m V^n |Y^{m,n}| sin(\theta^{m,n} + \delta^n - \delta^m), \quad (2)$$

where $\hat{P}^m, \hat{Q}^m$ are the real and reactive power injected at node m and δ^m is the voltage phase angle of the m-th DG. $\theta^{m,n}$ is the admittance angle. V^m is the local voltage magnitude and V^n is a neighboring voltage magnitude.

Remark 1: We assume the power lines in this microgrid are lossless as in [21] such that the line resistance is zero ($G^{m,n} = 0$). The work in [25] demonstrates how this assumption holds in microgrids; the basic argument is that while the resistance is non-negligible in medium and low voltage grids, the inverter output impedance is inductive enough to cause the resistance to be relatively small enough. This reduces the line impedances, $Y^{m,n} = G^{m,n} + jB^{m,n}$, to $Y^{m,n} = jB^{m,n}$.

As a result, the equations of state, (1) and (2), reduce to:

$$\hat{P}^m = \sum_{n\in\mathcal{N}_m} V^m V^n |B^{m,n}| sin(\delta^m - \delta^n) \tag{3}$$

$$\hat{Q}^m = (V^m)^2 \sum_{n\in\mathcal{N}_m} |B^{m,n}| - \sum_{n\in\mathcal{N}_m} V^m V^n |B^{m,n}| cos(\delta^m - \delta^n) \tag{4}$$

For tractability, we take $(\delta^m - \delta^n)$ to be very small such that the trigonometric small-angle approximations hold. The simplified power injection at a node is given as:

$$\hat{P}^m = \sum_{n\in\mathcal{N}_m} V^m V^n |B^{m,n}| (\delta_m - \delta_n) \tag{5}$$

$$\hat{Q}^m = (V^m)^2 \sum_{n\in\mathcal{N}_m} |B^{m,n}| - \sum_{n\in\mathcal{N}_m} V^m V^n |B^{m,n}| \tag{6}$$

B. Primary Control

The control of electric power systems is traditionally divided into three levels operating on different time scales. Droop-control is the classical primary controller, which operates on the fastest timescales and without communication requirements at each generation node in a network. Droop control uses a proportional gain acting on the real or reactive power to regulate the frequency or voltage, respectively. Namely, at the m-th DG:

$$\dot{\delta}^m = \omega^{ref} - n_{P^m}(P^{gen,m} - P^{ref,m}) \tag{7}$$

$$\dot{V}^m = V^{ref} - n_{Q^m}(Q^{gen,m} - Q^{ref,m}) \tag{8}$$

where $(*)^{ref}$ is the target for the variable (i.e. frequency, voltage, real and reactive power). The generation terms, $(*)^{gen}$, are then expanded to represent the loads, $(*)^{L,m}$, and injected power, $\hat{(*)}^m$:

$$P^{gen,m} = P^{L,m} + \hat{P}^m \tag{9}$$

$$Q^{gen,m} = Q^{L,m} + \hat{Q}^m \tag{10}$$

C. Secondary Control

Secondary control operates on a slower timescale to restore the voltage and frequency in a network to the references. Voltage and frequency regulation are necessary components of secondary control in any electric power system but must be taken into particular consideration in scenarios with grid-forming inverters. In an autonomous microgrid, at least one inverter is grid-forming; in this paper, we make all of the inverters grid-forming. Steady-state deviations from the reference occur without secondary control [20], [22].

The proportional controller illustrated in (7) deviates from the references since it has no integral action. In order to compensate for this, secondary controllers provide integral action to drive the quantities to their respective references; this must be achieved in finite time and the voltages, as local quantities, must be synchronized. In the distributed context, the necessity of information exchange between nodes is based on the latter requirement. The grid-forming inverter's internal voltage and virtual impedance drive the secondary voltage control input, as detailed in [26]. In consideration of space, we leave out further frequency-real power equations: we do not address frequency-real power in this work. The equation governing voltage is derived from (5), (7):

$$\begin{aligned}\tau_{Q^m}\dot{V^m} = &- V^m + V^{m,ref} + u^{V,m} \\ &- n_{Q^m}\Big(Q^{L,m} + (V^m)^2 \sum_{n\in\mathcal{N}_m} |B^{m,n}| - \\ &\sum_{n\in\mathcal{N}_m} V^m V^n |B^{m,n}| - Q^{ref,m}\Big),\end{aligned} \tag{11}$$

where τ_{Q_m} is the time constant associated with the voltage dynamics and $u^{V,m}$ is the secondary voltage control input, which comes from the VSI. In order to run this on a digital system, we discretize (11). A one-step Euler discretization, with sample time T_s, gives the following result and we subsume the voltage reference by the secondary control input:

$$\begin{aligned}V^m_{k+1} = &V^m_k + T_s\Bigg(- V^m_k + u^{V,m}_k \\ &- n_{Q^m}\Big(Q^{L,m}_k + (V^m_k)^2 \sum_{n\in\mathcal{N}_m} |B^{m,n}| \\ &- \sum_{n\in\mathcal{N}_m} V^m_k V^n_k |B^{m,n}| - Q^{ref,m}\Big)\Bigg)\end{aligned} \tag{12}$$

Due to imperfect knowledge of the system dynamics, particularly in the reactive power as a time-varying parameter, for now we introduce a known disturbance (found in Section IV) to the dynamics, d_k, giving:

$$\begin{aligned}V^m_{k+1} = &V^m_k + T_s\Bigg(- V^m_k + u^{V,m}_k \\ &- n_{Q^m}\big(Q^{L,m}_k + (V^m_k)^2 \sum_{n\in\mathcal{N}_m} |B^{m,n}| \\ &- \sum_{n\in\mathcal{N}_m} V^m_k V^n_k |B^{m,n}| - Q^{ref,m}_k + d_k\big)\Bigg)\end{aligned} \tag{13}$$

$$d_{k+1} = d_k \tag{14}$$

$$V^n_{k+1} = V^n_k, \qquad \forall n \in \mathcal{N}_{C_m} \tag{15}$$

We introduce (15) because the evolution of the neighbors' dynamics are difficult to model due to dynamical coupling; as such, we allow them to remain constant for the prediction horizon. Similarly, we consider (14) constant for the prediction horizon as the disturbance dynamics are unknown for now; various models can be used to model these quantities including momentum-based and distribution-based methods. These are left for future work.

III. Distributed Secondary Control for Voltage Restoration

We formulate the secondary voltage controller as a distributed nonlinear model predictive control (DNMPC) tracking problem, $\mathcal{P}^m$, where the problem is solved at each node with access to only its neighbors' voltage magnitudes and its own. For this work, the low level control anticipates new lower level control strategies that are distributed; this

distributed voltage controller would be implemented with a distributed frequency controller. The dynamics are left in the nonlinear form (13) in order to minimize the model mismatch. The distributed controller comes from the reliance on neighbors' state information, particularly V^n, $\forall n \in \mathcal{N}_m$ where for simplicity $\mathcal{N}_m = \mathcal{N}_{C_m}$. Thus, at every time step a node must communicate its current state to its neighbors. The hierarchical control consists of the low-level droop (proportional) control with a linear state feedback law that has implicit integral action for disturbance rejection. This optimization problem is an MPC formulation with some control horizon, H_u, and a prediction horizon H_p. Because modeling the neighbors' dynamical evolution is challenging due to dynamical coupling, we choose a fairly short prediction horizon (here we choose $H_p = 2$). The benefit of increasing H_p is small as the neighbors are modeled to be constant within H_p. The control horizon is chosen as $H_u = 1$. The controlled state is the local voltage.

We define the constraints for the problem as simply box constraints on the state as well as the initialization condition common to most MPC formulations. An input constraint is left off here as it is generally inactive for this problem. In particular, the network voltage is bounded above and below by acceptable limits. A common standard (ANSI C84.1) dictates staying within five percent of nominal:

$$0.95V^{ref} \leq V_k^m \leq 1.05V^{ref} \tag{16}$$

Given these constraints, define:

$$\mathcal{P}^m = \min_{u^m_{t+k|t}} \sum_{k=0}^{H_p} \left\|L(m,:)\mathbf{V_{t+k|t}}\right\|_Q^2 + \left\|V^m_{t+k|t} - V^{ref,m}_{t+k|t}\right\|_W^2 + \sum_{k=0}^{H_p-1} \left\|u^m_{t+k|t} - u^{ref,m}_{t+k|t}\right\|_R^2 \tag{17}$$

$$\text{s.t. (13)-(16)} \tag{18}$$

$$\mathbf{V}_{t|t} = \mathbf{V}(t) \tag{19}$$

Here, let $\|*\|_M^2 = (*)^T M(*)$. The notation $V^m_{t+k|t}$ denotes "the state at time $t+k$ predicted at time t" and $u^m_{t+k|t}$ denotes "the input at time $t+k$ computed at time t" [27]. The cost function of the DNMPC formulation is quadratic in three terms. The first term penalizes the difference between the local voltage and the neighbors' voltages. We express this as the inner product of the m-th row of the Laplacian, L, and the voltage vector, $\mathbf{V_{k+1}}$, letting unknown voltages be zero. This enables voltage synchronization. As a dynamically coupled state, the voltages should restore synchronously in order to avoid noisy transient responses (e.g. restoring one node's voltage asynchronously will result in readjusting when another node restores its voltage asynchronously). The second term penalizes the difference between the local voltage and the reference. The third term drives the control input towards the reference secondary voltage input. We take the terminal cost to be quadratic and of the same weight as prior costs such that it is included in the cost summation over H_p. Generally speaking, for linear systems, the references, $(*)^{ref}$, can be found via least squares [27].

A. Reference Computation

In order to compute the reference (or target) values, $u^{ref,m}_{t+k|t}$ and $V^{ref,m}_{t+k|t}$, for this nonlinear system, we extend the method for linear systems in [27] under stated assumptions. Let $x(t)^m$ generally denote the local state of the digital control system outside of the MPC. Consider the nonlinear system given in (13), written more generally as $x(t+1)^m = g(x(t)^m, u(t)^m, d(t)^m)$, with input $u(t)^m$ and disturbance $d(t)^m$, and measurement $z(t)^m = h(x(t)^m)$. Suppose the observer of the stochastic process $\hat{x}(t+1)^m = g(\hat{x}(t)^m, u(t)^m, v(t)^m, \hat{d}(t)^m)$, $z(t)^m = h(x(t)^m, w(t)^m)$, with process noise $v(t)^m$ and measurement noise $w(t)^m$, is stable. For now, let $w(t)^m, v(t)^m$, and $d(t)^m$ be known. In Section IV, these values will be determined. Furthermore, the number of outputs equals the dimension of the constant disturbance. Then, the steady-state observer, where $(*)_\infty$ denotes steady-state, satisfies,

$$\hat{x}^m_\infty = g(\hat{x}^m_\infty, u^m_\infty, v^m_\infty, \hat{d}^m_\infty) \tag{20}$$

$$z^m_\infty = h(\hat{x}^m_\infty, w^m_\infty) \tag{21}$$

This suggests that, if $z^m_\infty = z^{ref,m}$:

$$\hat{x}^{ref,m}_\infty = g(\hat{x}^{ref,m}_\infty, u^{ref,m}_\infty, v^m_\infty, \hat{d}^m_\infty) \tag{22}$$

$$z^{ref,m} = h(\hat{x}^{ref,m}_\infty, w^m_\infty) \tag{23}$$

At steady-state, $u^{ref,m}_\infty$ and $\hat{x}^{ref,m}_\infty$ can be found by solving the system of equations in (22), (23). If the closed-loop system converges to $x^{ref,m}_\infty, d^m_\infty, z^{ref,m}$, then the intuitive argument is that, $u(t)^{ref,m}$ can be found at steady-state since $x(t+1)^{ref,m} = x(t)^{ref,m}$. Then, in the region of the reference, $\bar{x}(t)^{ref,m} := x(t+1)^{ref,m} \approx x(t)^{ref,m}$ such that:

$$\bar{x}(t)^{ref,m} = g(\bar{x}(t)^{ref,m}, u^{ref,m}(t), v(t)^m, d(t)^m) \tag{24}$$

$$z(t)^m = h(\bar{x}(t)^{ref,m}, w(t)^m) \tag{25}$$

Then, as $z(t)^m \to z^m_\infty = z^{ref,m}$ and $x(t) \to x^{ref,m}_\infty$, $u^{ref,m}(t) \to u^{ref,m}_\infty$ as $t \to \infty$.

Note the reference input for step k in the prediction horizon H_p is time-invariant since the neighbors' states and the local disturbance are constant as well. For the dynamics in this work, the targets are computed under the assumption that $\exists(u^{ref,m}, \hat{x}^{ref,m})$ satisfying (20). This assumption holds under the test conditions because the MPC is persistently feasible–without this, the references can still be computed under nonlinear least squares methods such as Newton-Gauss iteration. The steady-state form of the observer for this problem's dynamics (12) suggests the targets can be computed analytically. In particular, the observer at steady-

state yields:

$$\begin{aligned}\hat{V}_{\infty}^{ref,m} =&\hat{V}_{\infty}^{ref,m} + T_s\Bigg(- \hat{V}_{\infty}^{ref,m} + u_{\infty}^{ref,m} \\ &- n_{Q^m}\Big(Q_{\infty}^{L,m} + (\hat{V}_{\infty}^{ref,m})^2 \sum_{n\in\mathcal{N}_m} |B^{m,n}| \\ &- \sum_{n\in\mathcal{N}_m} \hat{V}_{\infty}^{ref,m}\hat{V}_{\infty}^{n}|B^{m,n}| - Q_{\infty}^{ref,m} \\ &+ \hat{d}_{\infty} + v_{\infty,1}^{m}\Big)\Bigg) \\ z_{\infty}^{ref,m} =&\hat{V}_{\infty}^{ref,m}\end{aligned} \tag{26}$$

We solve this for input reference, $u_{\infty}^{ref,m}$. Trivially, $V_{\infty}^{ref,m}$ is the measured value. This can be extended for all time, t, such that:

$$\begin{aligned}u(t)^{ref,m} =&\hat{V}(t)^{ref,m} + n_{Q^m}\big(Q(t)^{L,m} \\ &+ (\hat{V}(t)^{ref,m})^2 \sum_{n\in\mathcal{N}_m} |B^{m,n}| \\ &- \sum_{n\in\mathcal{N}_m} \hat{V}(t)^{ref,m}\hat{V}(t)^{n}|B^{m,n}| \\ &- Q(t)^{ref,m} + \hat{d}(t)\big)\end{aligned} \tag{27}$$

Again, the state reference is just $V(t)^{ref,m}$, the desired nominal value. This target computation, with knowledge of the disturbances, results in $\mathcal{P}^m$ tracking the voltage references without offset as the system approaches steady-state and $u_{t+k|t}^{m} \to u_{t+k|t}^{ref,m}$. While this is the computation of the reference input and not the input itself, the actual input takes this form as it reaches steady state.

IV. Distributed State Estimation

Given $\mathcal{P}^m$, we must solve the practical problem of finding $d_{t|t}$. We propose an unscented Kalman filter (UKF) to estimate the disturbance to a given node. This observer allows for the preservation of the nonlinear dynamics but lacks a condition for stability. Define P_{noise}^{est} as the process noise covariance matrix and M_{noise}^{est} as the measurement noise covariance matrix. The dynamics of the estimator with non-additive process noise, $v(t)_l^m \in \mathcal{N}(0, P_{noise}^{est})$ $l = 1, 2$, and measurement noise, $w(t)^m \in \mathcal{N}(0, M_{noise}^{est})$, then becomes:

$$\begin{aligned}\hat{V}(t+1)^m =&\hat{V}(t)^m + T_s\Bigg(- \hat{V}(t)^m + u(t)^{V,m} \\ &- n_{Q^m}\Big(Q(t)^{L,m} + (\hat{V}(t)^m)^2 \sum_{n\in\mathcal{N}_m} |B^{m,n}| \\ &- \sum_{n\in\mathcal{N}_m} \hat{V}(t)^m V(t)^n|B^{m,n}| \\ &- Q(t)^{ref,m} + \hat{d}(t) + v(t)_1^m\Big)\Bigg)\end{aligned} \tag{28}$$

$$\hat{d}(t+1) = \hat{d}(t) + v(t)_2^m \tag{29}$$

$$V(t)^{meas,m} = \hat{V}(t)^m + w(t)^m \tag{30}$$

Here we denote the estimated states as $\hat{(*)}$. The noises have subscripts to indicate the element of the vector. The random-walk disturbance estimation method was proposed in [28]. By including the process noise disturbance with the unmeasured disturbance (29), the evolution of the disturbance is a random walk resulting in a non-zero mean estimate of the disturbance. When considering whether this is observable, the estimator was merely demonstrated to work and mathematical proof of this for the nonlinear dynamics is left for future work. However, we note that the linearized system around the reference is observable.

The UKF allows for transient disturbances to be tracked with some delay due to the continuity of a random walk and potential step responses in the applied disturbances. The UKF as an observer then interfaces with the DNMPC where the state inputs to $\mathcal{P}^m$ become $\hat{V}(t)^m, \hat{d}(t)$. Through simulation, we demonstrate the observer to be stable under tested conditions and the DNMPC is as well. Note the UKF and DMPC are run in series instead of parallel, which accounts for the stochasticity of the problem outside of the MPC. The work in [29] also uses this series coupling such that the evolution of each prediction horizon is deterministic.

V. Simulation

A. Simulation Environment

In order to test the methods discussed in Sections III, IV, we create two simulation environments. Both environments have a four node radial network as shown in Fig. 1. We implement the same controller in both instances with just the plant subsystem changing. We instantiate the DNMPC in a fully-distributed sense so that the independence of the subsystems is immediately clear. We encode the controller as an Interpreted MATLAB Function containing (17) written with YALMIP [30] using the solver GUROBI or IPOPT. We use rate transition blocks (zero-order hold and inverse zero-order hold throughout the network for interfacing continuous and discrete time components). The stiff system requires the use of the continuous time integrator *ode23s*.

1) Model perfect: We use Simulink blocks to create a four-node network (Table I) in the first simulator. This shows the applicability of (17) to a continuous-time dynamical system. The first order ODE (11) is fully-represented with non-additive process noise, measurement noise, and time-varying and time-invariant disturbances.

The pure Simulink parameters are from [21] for a single phase (Table I).

B. Simulation Results

The framework indicates the overall viability of the control scheme. We include the test cases and parameters in Table I, II. We tune the UKFs according to the test case with the means, distributions, and covariance matrices generally assumed to be known. We tabulate the specific values in Table II. We leave the UKF parameters α, β, κ at the nominal values indicated.

1) Test Case 1: The controller with UKF in series is simulated (Fig. 2) for the model perfect simulator. The resulting data (horizon truncated for visibility) indicates that the closed-loop system is stable for the chosen parameters.

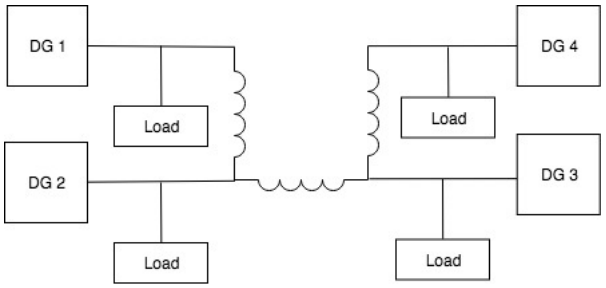

Fig. 1. Four-node MG

TABLE I

SIMULINK PARAMETERS TO TEST THE CONTROLLER

Parameter	DG1	DG2	DG3	DG4
Q^{ref}	1e4	1e4	1e4	1e4
Q^{load}	1e4	1e4	1e4	1e4
n_{Q^m}	4.24e-4	4.24e-4	4.24e-4	4.24e-4
d^m	-5e3	-2e3	-1e3	-3e3
Cost		$Q = 10I$	$W = 5I$	$R = 1I$
B (Ω^{-1})		B_{12} = 10	B_{23} = 10.67	B_{34} = 9.82
V^{ref}		$310V$		
τ_{Q_m}, T_s (sec)		0.016, 0.03		

TABLE II

THE TEST PARAMETERS FOR THE TWO CASES.

Case	P_{noise}	P^{est}_{noise}	M_{noise}	M^{est}_{noise}
1	$\begin{bmatrix} 1e\text{-}3 & 0 \\ 0 & 0 \end{bmatrix}$	$\begin{bmatrix} 1e\text{-}3 & 0 \\ 0 & 1e2 \end{bmatrix}$	1e-1	1e-1
2	$\begin{bmatrix} 1e\text{-}1 & 0 \\ 0 & 0 \end{bmatrix}$	$\begin{bmatrix} 1e\text{-}1 & 0 \\ 0 & 1e3 \end{bmatrix}$	1	1
UKF	α = 1e-1	β = 2 (Gaussian)		$\kappa = 0$

The step response at $t = 30$ seconds for the first simulator indicates the secondary controller turning on in Fig. 2. The primary controller begins at $t = 0$ seconds and provides a stable system with offset. It can be seen that the UKF (initialized at $t = 0$ seconds) estimates the disturbances over time as the random walk allows the initial estimate to evolve to the actual value. The rate at which the UKF approaches the constant disturbance is a function of the variance of the disturbance state in (28). Higher variances increase the convergence rate but will increase the steady-state error as the estimation will always be distributed around the disturbance and never exactly at the constant disturbance.

2) Test Case 2: Here, we increase the process and measurement noise to observe the performance of the controller. The closed-loop system remains stable and the disturbance rejection is maintained. The effective integral action rejects the disturbances insofar as the disturbance is properly estimated; in Fig. 3, the estimator takes close to 180 seconds to reach the disturbance value. As a result, the voltage restoration can only reach the reference when the estimator reaches the actual disturbance value. The resiliency of the algorithm to noisy disturbances can be evaluated on the relative magnitude of the disturbance to expected reactive power,

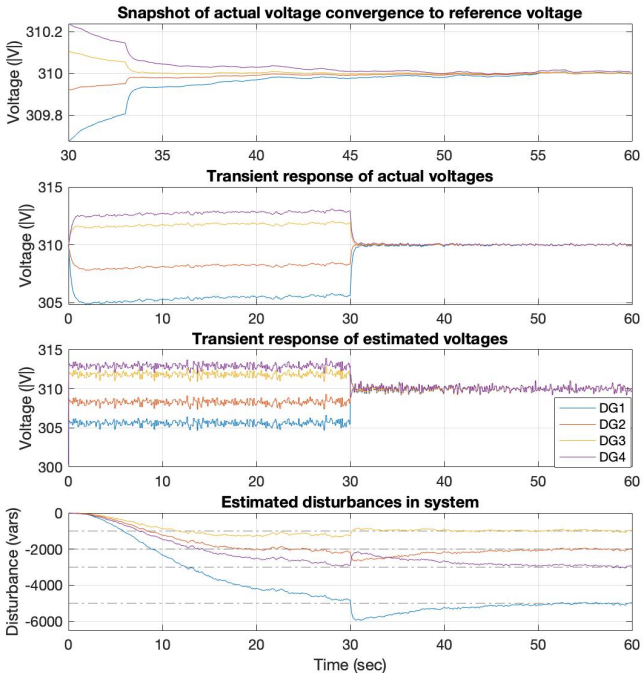

Fig. 2. Constant disturbance rejection with random walk estimator. The first subplot shows how the error goes to zero (with some transience due to noise) as the estimator goes to the constant disturbance value. The subplot of the disturbances shows how the estimator approaches the actual value and has a significant step when the secondary controller turns on.

Q^{ref}; here it is demonstrated with steady-state disturbances of up to 50% of the expected and Gaussian noise of up to 1e-3% of the expected.

VI. CONCLUSION AND FUTURE WORK

We propose a distributed nonlinear model predictive control formulation in this work to restore voltages in an inverter-based autonomous microgrid. Unlike previous work in secondary voltage control via MPC, which use simplified dynamics, the evolution of the local voltage is directly influenced by the neighbors' voltages, which allows for the realization of the impact of the neighbors' states. The estimator and MPC in series is novel in this context for estimating non-zero mean disturbances. In particular, unmeasured reactive power injection/consumption are estimated by using a random walk model; previous work did not account for model mismatch. From these estimates, we formulate a novel integral action using the full dynamics that admits an analytic solution instead of relying on least squares. Via simulation, we demonstrate the ability of these novel components to perform secondary control on the voltage.

By using the nonlinear form of the dynamics, model mismatches are less likely–therefore allowing for more focus to be on the estimation aspects of this work. For analysis and mathematical proofs, we are working on linearizing this approach. Benchmarks of the MPC formulation against policies computed offline will be included to establish the benefit of the receding horizon. Additionally, we can add the dynamics of the neighbors with some assumptions about

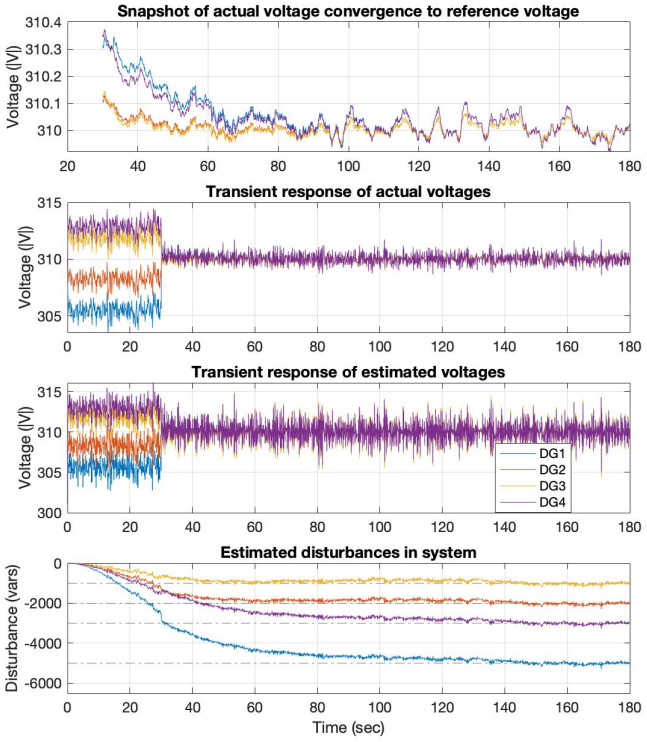

Fig. 3. High noise constant disturbance rejection with random walk estimator. We inject relatively high reactive power noise in this second case resulting in a noisy actual voltage, but the voltage still tracks the reference with transient minor offsets.

knowledge of the network graph and the neighbors' control inputs. Lastly, we can include modeling and controlling the frequency in future work.

REFERENCES

[1] M. Yazdanian and A. Mehrizi-Sani, "Distributed control techniques in microgrids," *IEEE Transactions on Smart Grid*, vol. 5, no. 6, pp. 2901–2909, Nov 2014.

[2] J. A. P. Lopes, C. L. Moreira, and A. G. Madureira, "Defining control strategies for microgrids islanded operation," *IEEE Transactions on Power Systems*, vol. 21, no. 2, pp. 916–924, May 2006.

[3] N. Pogaku, M. Prodanovic, and T. C. Green, "Modeling, analysis and testing of autonomous operation of an inverter-based microgrid," *IEEE Transactions on Power Electronics*, vol. 22, no. 2, pp. 613–625, March 2007.

[4] M. C. Chandorkar, D. M. Divan, and R. Adapa, "Control of parallel connected inverters in standalone ac supply systems," *IEEE Transactions on Industry Applications*, vol. 29, no. 1, pp. 136–143, Jan 1993.

[5] M. Glavic, "Power system voltage stability: A short tutorial."

[6] A. Bidram and A. Davoudi, "Hierarchical structure of microgrids control system," *IEEE Transactions on Smart Grid*, vol. 3, no. 4, pp. 1963–1976, Dec 2012.

[7] T. L. Vandoorn, J. C. Vasquez, J. De Kooning, J. M. Guerrero, and L. Vandevelde, "Microgrids: Hierarchical control and an overview of the control and reserve management strategies," *IEEE Industrial Electronics Magazine*, vol. 7, no. 4, pp. 42–55, Dec 2013.

[8] A. Bidram, V. Nasirian, A. Davoudi, and F. L. Lewis, "Control and modeling of microgrids," in *Cooperative Synchronization in Distributed Microgrid Control*. Springer, 2017, pp. 7–43.

[9] A. Kaur, J. Kaushal, and P. Basak, "A review on microgrid central controller," *Renewable and Sustainable Energy Reviews*, vol. 55, pp. 338–345, 2016.

[10] A. Pilloni, A. Pisano, and E. Usai, "Robust finite-time frequency and voltage restoration of inverter-based microgrids via sliding-mode cooperative control," *IEEE Transactions on Industrial Electronics*, vol. 65, no. 1, pp. 907–917, Jan 2018.

[11] O. Sondermeijer, R. Dobbe, D. Arnold, C. Tomlin, and T. Keviczky, "Regression-based inverter control for decentralized optimal power flow and voltage regulation," 2015.

[12] R. Dobbe, D. Fridovich-Keil, and C. Tomlin, "Fully decentralized policies for multi-agent systems: An information theoretic approach," in *Advances in Neural Information Processing Systems 30*, I. Guyon, U. V. Luxburg, S. Bengio, H. Wallach, R. Fergus, S. Vishwanathan, and R. Garnett, Eds. Curran Associates, Inc., 2017, pp. 2941–2950.

[13] E. J. Davison and T. N. Chang, "Decentralized stabilization and pole assignment for general proper systems," *IEEE Transactions on Automatic Control*, vol. 35, no. 6, pp. 652–664, 1990.

[14] P. D. Christofides, R. Scattolini, D. M. de la Pea, and J. Liu, "Distributed model predictive control: A tutorial review and future research directions," *Computers and Chemical Engineering*, vol. 51, pp. 21–41, 2013, cPC VIII. [Online]. Available: http://www.sciencedirect.com/science/article/pii/S0098135412001573

[15] J. M. Maestre and R. R. Negenborn, *Distributed Model Predictive Control Made Easy*. Springer Publishing Company, Incorporated, 2013.

[16] J. K. Yook, D. M. Tilbury, and N. R. Soparkar, "Trading computation for bandwidth: reducing communication in distributed control systems using state estimators," *IEEE Transactions on Control Systems Technology*, vol. 10, no. 4, pp. 503–518, Jul 2002.

[17] R. R. Negenborn and J. Maestre, "Distributed model predictive control: An overview and roadmap of future research opportunities," *IEEE Control Systems Magazine*, vol. 34, no. 4, pp. 87–97, 2014.

[18] S. Roshany-Yamchi, M. Cychowski, R. R. Negenborn, B. D. Schutter, K. Delaney, and J. Connell, "Kalman filter-based distributed predictive control of large-scale multi-rate systems: Application to power networks," *IEEE Transactions on Control Systems Technology*, vol. 21, no. 1, pp. 27–39, Jan 2013.

[19] H. Almasalma, J. Engels, and G. Deconinck, "Peer-to-Peer Control of Microgrids," *ArXiv e-prints*, Nov. 2017.

[20] C. Gang and G. Zhijun, "Distributed secondary control for droop-controlled autonomous microgrid," in *2015 34th Chinese Control Conference (CCC)*, July 2015, pp. 9008–9013.

[21] F. Guo, C. Wen, J. Mao, and Y. D. Song, "Distributed secondary voltage and frequency restoration control of droop-controlled inverter-based microgrids," *IEEE Transactions on Industrial Electronics*, vol. 62, no. 7, pp. 4355–4364, July 2015.

[22] G. Lou, W. Gu, Y. Xu, M. Cheng, and W. Liu, "Distributed mpc-based secondary voltage control scheme for autonomous droop-controlled microgrids," *IEEE Transactions on Sustainable Energy*, vol. 8, no. 2, pp. 792–804, April 2017.

[23] M. N. Zeilinger, Y. Pu, S. Riverso, G. Ferrari-Trecate, and C. N. Jones, "Plug and play distributed model predictive control based on distributed invariance and optimization," in *52nd IEEE Conference on Decision and Control*, Dec 2013, pp. 5770–5776.

[24] J. Grainger and W. Stevenson, *Power System Analysis*, ser. McGraw-Hill series in electrical and computer engineering: Power and energy. McGraw-Hill Education, 2016. [Online]. Available: https://books.google.com/books?id=ddSAjwEACAAJ

[25] J. Schiffer, R. Ortega, A. Astolfi, J. Raisch, and T. Sezi, "Conditions for stability of droop-controlled inverter-based microgrids," *Automatica*, vol. 50, no. 10, pp. 2457–2469, 2014.

[26] J. Rocabert, A. Luna, F. Blaabjerg, and P. Rodrguez, "Control of power converters in ac microgrids," *IEEE Transactions on Power Electronics*, vol. 27, no. 11, pp. 4734–4749, Nov 2012.

[27] F. Borrelli, A. Bemporad, and M. Morari, *Predictive Control for Linear and Hybrid Systems*. Cambridge University Press, 2011, pp. 251, 273–279.

[28] D.-W. Kim and C.-S. Park, "Application of kalman filter for estimating a process disturbance in a building space," *Sustainability*, vol. 9, no. 10, 2017. [Online]. Available: http://www.mdpi.com/2071-1050/9/10/1868

[29] H. Yu, J. Duan, S. Taheri, H. Cheng, and Z. Qi, "A model predictive control approach combined unscented kalman filter vehicle state estimation in intelligent vehicle trajectory tracking," *Advances in Mechanical Engineering*, vol. 7, no. 5, p. 1687814015578361, 2015. [Online]. Available: https://doi.org/10.1177/1687814015578361

[30] J. Löfberg, "Yalmip : A toolbox for modeling and optimization in matlab," in *In Proceedings of the CACSD Conference*, Taipei, Taiwan, 2004.